DELPHI 97-108 CONF 90
28 July, 1997

Measurement of the W-pair cross-section and of the W mass in e^+e^- interactions at 172 GeV

Preliminary

DELPHI Collaboration

P.Buschmann[1], M.Bigi[2], M.Calvi[3], V.Canale[4], R.Chierici[2], D.Fassouliotis[5], P.Jarry[6], N.J.Kjaer[7], G.Matthiae[4], R.Moller[8], K.Mönig[9], M.Mulders[7], G.Orazi[10], A.Ouraou[6], M.Paganoni[9], C.Parkes[11], P.Privitera[4], P.Renton[11], J.Thomas[11], M.L.Turluer[6], J.Timmermans[7], A.Tonazzo[3], V.Verzi[4], H.Wahlen[1], G.Wilkinson[9]

Abstract

From a data sample of 9.98 pb^{-1} integrated luminosity, collected by DELPHI at a centre-of-mass energy of 172 GeV, 118 events were selected as W-pair candidates. From these, the branching ratio $Br(W \to q\bar{q})$ was measured to be $0.660^{+0.036}_{-0.037}(stat.) \pm 0.009(syst.)$ and the cross-section for the doubly resonant process $e^+e^- \to W^+W^-$ to be $11.58^{+1.44}_{-1.35}(stat.) \pm 0.32(syst.)$ pb. The mass of the W boson has been obtained from direct reconstruction of the invariant mass of the fermion pairs in the decays $WW \to \ell\nu q\bar{q}$ and $WW \to q\bar{q}q\bar{q}$: $m_W = 80.22 \pm 0.41(stat.) \pm 0.04(syst.) \pm 0.05(int.) \pm 0.03(LEP)\, GeV/c^2$, where int. denotes the error from interconnection effects like colour reconnection and Bose-Einstein interference. Combined with the W mass obtained from the cross-sections measured by DELPHI, a value of $m_W = 80.33 \pm 0.30(stat.) \pm 0.05(syst.) \pm 0.03(int.) \pm 0.03(LEP)\, GeV/c^2$ is found.

Paper submitted to the LP'97 Conference
Hamburg, July 28 - August 1st

[1]Fachberich Physik, University of Wuppertal, Postfach 100 127, D-42097 Wuppertal, Germany
[2]Dip. di Fisica Sperimentale, Università di Torino and INFN, via P.Giuria 1, I-10125 Turin, Italy
[3]Dipartimento di Fisica, Università di Milano and INFN, via Celoria 16, I-20133 Milan, Italy
[4]Dipartimento di Fisica, Università di Roma II and INFN, Tor Vergata, I-00173 Rome, Italy
[5]Dipartimento di Fisica, Università di Trieste and INFN, Via A. Valerio 2, I-34127 Trieste, Italy
[6]CEA, DAPNIA/Service de Physique des Particules, CE-Saclay, F-91191 Gif-sur-Yvette Cedex, France
[7]NIKHEF, Postbus 41882, NL-1009 DB Amsterdam, The Netherlands
[8]Niels Bohr Institute, Blegdamsvej 17, DK-2100 Copenhagen 0, Denmark
[9]CERN, CH-1211 Geneva 23, Switzerland
[10]Centre de Recherche Nucléaire, IN2P3-CNRS/ULP-BP20, F-67037 Strasbourg Cedex, France
[11]Department of Physics, University of Oxford, Keble Road, Oxford OX1 3RH, UK

1 Introduction

In autumn of 1996, LEP provided e^+e^-collisions at a centre-of-mass energy of 170.3 and 172.3 GeV. DELPHI collected data corresponding to a total integrated luminosity of 9.98 pb^{-1} at a luminosity weighted average energy of 172.14 GeV. At these energies the ratio of the expected cross-section for W-pair production to the background is about a factor four higher than at threshold. The sensitivity of the W-pair production cross-section to the W mass is however much reduced, compared to the cross-section at threshold. Instead, at these higher energies, the measurement of the W mass can be made by direct reconstruction of the invariant mass of the fermion pairs from each W decay, using constrained fitting techniques.

This paper is organized as follows. In section 2, the DELPHI detector setup in 1996, the event trigger, and the luminosity measurement are briefly reviewed. The track selection and lepton identification are described in section 3. In section 4, the event selection and the computation of cross-sections are presented for the different decay channels, from which the branching ratio $\mathrm{Br}(\mathrm{W} \to \mathrm{q\bar{q}})$ and the total cross-section are derived. The measurements of the W mass from direct reconstruction are given in section 5. Finally, a combined value for m_{W} from direct reconstruction and from the WW threshold cross-section [1] is given in section 6.

2 Apparatus, Trigger and Luminosity

Detailed descriptions of the DELPHI apparatus and its performance can be found in [2, 3]. In 1996 the cylindrical 3-layer vertex detector was lengthened and extended with additional silicon detectors covering the endcap region.

The response of the detector to various physics processes was modelled using the full simulation program DELSIM [3, 4], which incorporates the resolution, granularity, and efficiency of the detector components. The event generators chosen are described in the relevant sections below.

The event trigger is described in [2, 3]. From trigger efficiencies measured for single charged particles with redundant trigger combinations, the efficiency for two charged particles (which is the worst case for all events of interest in the present analysis) was found to exceed 99%.

The luminosity was measured using the Small Angle Tile Calorimeter (STIC). It consists of two lead/scintillator sampling calorimeters, located at $\pm$ 220 cm from the interaction point, providing full coverage of the region between 29 and 185 mrad with respect to the beam axis. A detailed description of this detector can be found in [5]. Events corresponding to Bhabha scattering were selected by requiring a coincidence of two coplanar electromagnetic showers, each with energy larger than 65% of the beam energy. In order to minimize the sensitivity to the position of the interaction point, asymmetric cuts were imposed on the reconstructed radii of the two showers.

The calculation of the accepted cross-section was based on the event generator BHLUMI 4.03 [6], which has a theoretical accuracy of 0.25% at LEP2 energies. The generated events were passed through a full simulation of the detector, and analysed in the same way as the real data. The total experimental systematic error on the luminosity amounts to 0.5%, with the main contribution arising from the uncertainty in the radial cuts. For the data sample used, an integrated luminosity of $9.98 \pm 0.05(\mathrm{stat.}) \pm 0.06(\mathrm{syst.})\ \mathrm{pb}^{-1}$ was determined.

3 Track Selection and Lepton Identification

Charged particles were selected if they fulfilled the following criteria :

- polar angle with respect to the beam direction between 10° and 170°;
- momentum greater than 0.4 GeV/c;
- good quality, assessed as follows:
  - track length greater than 15 cm;
  - impact parameters with respect to the nominal interaction point less than 4 cm (transverse and longitudinal with respect to the beam direction);
  - estimated relative error on momentum measurement less than 100%.

For neutral particles the following selection criteria were applied :

- energy of the shower greater than 0.5 GeV;
- additional requirements on shower quality, assessed as follows:
  - showers in the STIC calorimeter with deposits in more than one cell;
  - showers in the hadron calorimeter with energy uncertainties below 100%.

Electron identification was performed in the polar angle range between 20° and 160° by looking for charged particles with a characteristic energy deposition in the central and forward/backward electromagnetic calorimeters. For this polar angle range the identification efficiency for high energy electrons was determined from simulation to be $(77 \pm 2)\%$, in good agreement with efficiencies determined using Bhabha events measured in the detector.

Tracks were identified as due to muons if they had at least one associated hit in the muon chambers, or an energy deposition in the hadronic calorimeter consistent with a minimum ionizing particle. Muon identification was performed in the polar angle range between 10° and 170°. Within this acceptance, the identification efficiency was determined from simulation to be $(92 \pm 1)\%$. Good agreement was found between data and simulation for high momentum muons in $\mathrm{Z} \to \mu^+\mu^-$ decays, and for low momentum pairs produced in $\gamma\gamma$ reactions.

4 Event Selection and Cross-Sections

The analysis described here is similar to the one used for the measurement of the threshold cross-section at 161.3 GeV [1]. At 172 GeV, the ratio of the signal cross-section to the cross-section of Z/γ events is about four times larger than at threshold. This allows some of the cuts to be relaxed and improves the efficiency of the selections. Other selection cuts are rescaled in accordance with the increase in total energy.

The cross-sections determined in this analysis are defined to correspond to W pair production through the three doubly resonant tree-level diagrams ("CC03 diagrams" [7]) involving s-channel γ and Z exchange and t-channel ν exchange. The selection efficiencies given in this section are also defined with respect to these diagrams only. Depending on the decay mode of each W, fully hadronic, mixed hadronic-leptonic ("semileptonic"), or fully leptonic final states are obtained. The Standard Model branching ratios are 45.9%, 43.7% and 10.4% respectively. In addition to their production via the CC03 diagrams, the four-fermion final states corresponding to these decay modes may be produced via other diagrams involving either zero, one, or two massive vector bosons. The effects of the interference between the CC03 diagrams and the additional diagrams have been treated as correction factors [1], which were applied such that the cross-sections given below can be compared to theoretical estimates of the CC03 cross-sections. The numerical values of these correction factors at a centre-of-mass energy of 172 GeV are given in table 1. The uncertainties are estimated to be about 1.5% and are taken into account in the systematic uncertainties on the cross-sections given below. The correction factors are consistent with unity within errors.

WW decay mode	C_{CC03}
$\mathrm{q\bar{q}q\bar{q}}$	0.980
$\mathrm{e}\nu\mathrm{q\bar{q}}$	1.019
$\mu(\tau)\nu\mathrm{q\bar{q}}$	0.996
$\ell\nu\ell\nu$	0.980

Table 1: Correction factors C_{CC03} for the decay modes of WW pairs. For $\ell\nu\ell\nu$ the correction factor given is the combined value for all lepton combinations.

4.1 Fully Hadronic Final State

The event selection criteria were optimized in order to ensure that the final state was purely hadronic and in order to reduce the residual background. The background is dominated by electron-positron annihilation into $\mathrm{q\bar{q}}(\gamma)$, with a cross-section about one order of magnitude larger than that for the signal.

For each event, all particles were clustered into jets using the LUCLUS algorithm [8] with $d_{join} = 6.0$ GeV$/c$. At least 4 jets were required, with at least four particles in each jet. Events coming from the radiative return to the Z peak were rejected by requiring $\sqrt{s'} > 100$ GeV. $\sqrt{s'}$ is a measure of the effective collision energy after initial state radiation [9].

Events were then forced into a 4-jet configuration, and a kinematically constrained fit performed, imposing energy and momentum conservation. For the separation of WW events and $\mathrm{q\bar{q}}(\gamma)$ events the variable D is used:

$$D = \frac{E_{min}}{E_{max}} \cdot \frac{\theta_{min}}{(E_{max} - E_{min})} \tag{1}$$

where E_{min}, E_{max} are the energies of the jets with least and greatest energy, and θ_{min} is the smallest interjet angle, after the constrained fit. D was required to exceed 0.004 GeV^{-1}. Figure 1 shows the distribution of this quantity after the other cuts described above.

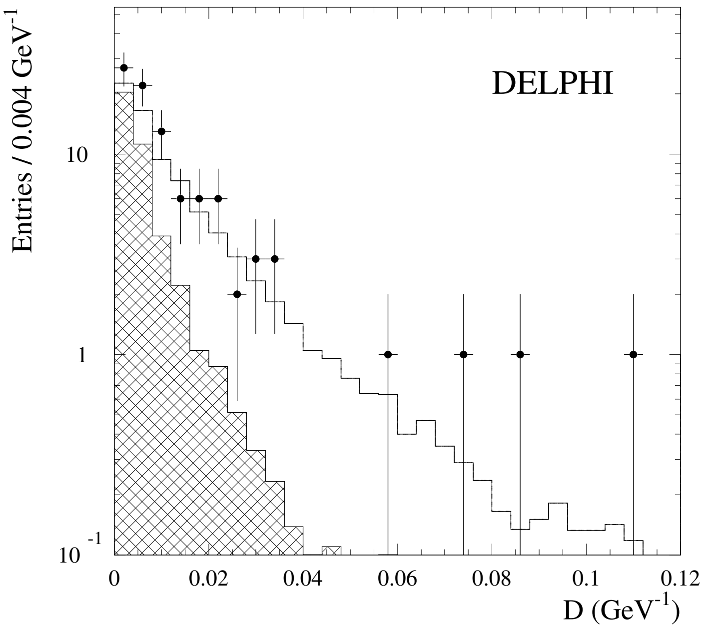

Figure 1: Distribution of the D variable (as defined in the text) for 4-jet events with effective centre-of-mass energy greater than 100 GeV. The data (points with error bars) are compared with simulated $q\bar{q}(\gamma)$ background (cross-hatched areas) and WW signal (white areas) normalised to the fitted cross-section.

The selection efficiency was computed from a sample of WW events generated with the generator PYTHIA 5.7 [10] (with $m_W = 80.35$ GeV/c^2), with the fragmentation tuned to the DELPHI data measured at LEP1 [11] and passed through the full DELPHI simulation. It was found to be $(82.7 \pm 1.6)\%$. The error includes the systematic uncertainty, which was estimated by varying all selection criteria by at least the value of their experimental resolutions and taking the quadratic sum of all contributions.

A residual background cross-section of 2.14 ± 0.16 pb was estimated, with the dominant contribution coming from e^+e^- annihilation into $q\bar{q}(\gamma)$ events, 1.6% of which survived the WW selection procedure, corresponding to a residual cross-section of 1.96 pb. The other contributions come from the channel $e^+e^- \to ZZ$ (0.11 pb) and the semileptonic final states of $e^+e^- \to W^+W^-$ (0.06 pb), while the background from $e^+e^- \to Ze^+e^-$ is negligible. The systematic uncertainty on the background was estimated from the variation of the selection efficiency for the $q\bar{q}(\gamma)$ background using different generators. Furthermore the accuracy of the simulation was checked on multihadronic events collected at the Z pole. These data were selected with the 172 GeV criteria downscaled in proportion to the collision energy, and good agreement was found with the expected numbers of events.

From the full data sample, 65 events were selected. The cross-section for fully hadronic events is obtained from a binned maximum likelihood fit to the distribution of the variable D for $D > 0.004$, taking into account the expected background in each bin. The result is

$$\sigma_{\mathrm{WW}}^{q\bar{q}q\bar{q}} = \sigma_{\mathrm{WW}}^{tot} \times \mathrm{Br}(\mathrm{WW} \to \mathrm{q\bar{q}q\bar{q}}) = 4.74^{+0.95}_{-0.86} \pm 0.18 \text{ pb},$$

where $\mathrm{Br}(\mathrm{WW} \to \mathrm{q\bar{q}q\bar{q}})$ is the probability for the WW pair to give a purely hadronic final state, and the first error is statistical and the last is systematic. The dominant contribution to the systematic error (0.15 pb) comes from the uncertainty on the background. The other components are due to the uncertainties in the efficiency, CC03 factor and luminosity.

4.2 Semileptonic Final States

Events in which one W decays into $\ell\nu$ and the other into quarks are characterized by two hadronic jets, one isolated lepton (coming either from W decay or from the cascade decay $\mathrm{W} \to \tau\nu \to \ell X$) or a low multiplicity jet due to τ decay, and a missing momentum resulting from the neutrino(s). The major background comes from $q\bar{q}(\gamma)$ production and from four-fermion final states containing two quarks and two leptons of the same flavour.

The events were required to contain at least 6 charged particles with total energy of at least $0.15\,E_{cms}$. Events with a detected initial state radiation photon of energy > 30 GeV were rejected. In the case of WW decays into $q\bar{q}\mu\nu$ and $q\bar{q}e\nu$ the candidate lepton was required to be the most energetic charged particle in the event, while the τ candidates were selected by looking for an isolated e or μ or a jet of multiplicity ≤ 5 with ≤ 3 charged particles and total momentum > 10 GeV/c.

Muon candidates were selected using information from the muon chambers and from the hadron calorimeter. The candidates were required to have momentum > 5 GeV/c, and the isolation angle between the candidate muon and the nearest charged particle with momentum > 1 GeV/c was required to exceed a value set between 8° and 20°, depending on the quality of the muon identification.

Electron identification was performed by looking for tracks of charged particles with energy deposits in the electromagnetic calorimeters matching the particle momentum within 20%, or exceeding 20 GeV. The momentum of the electron was required to be > 5 GeV/c and the component of the missing momentum transverse to the beam axis, p^t_{miss}, was required to exceed 10 GeV/c. The isolation angle between the candidate electron and the nearest charged particle with momentum above 1 GeV/c was required to exceed a value between 5° and 20°, depending on the quality of the electron identification.

In order to increase the efficiency of the selection, cases where the candidate was either not isolated or not identified as a lepton were also treated. The kinematic requirements in this case were tighter, rejecting events if the angle between the direction of the missing momentum and the beam axis was $< 18^\circ$ (30° for identified electrons) or if $\sqrt{s'}$ was $> E_{cms} - 15$ GeV.

The four-fermion background ($q\bar{q}\ell\ell$) was suppressed by applying an additional cut to the events in which a second lepton of the same flavour and with a charge opposite to that of the candidate was found. The event was rejected if the second lepton had a momentum above 5 GeV/c and an isolation angle with respect to all the other particles except the candidate lepton above 15°.

In the selection of $q\bar{q}\tau\nu$ events with the τ decaying hadronically, the events were only accepted if at least 3 jets (found using the LUCLUS [8] algorithm with $d_{join} = 3$ GeV/c) were reconstructed, and if the missing energy and the transverse energy both exceeded 40 GeV. Due to the fact that the $q\bar{q}(\gamma)$ background is concentrated in two regions of $\sqrt{s'}$, while the signal is randomly distributed in between, the kinematic requirements described above were tightened in the unfavourable regions (for $\sqrt{s'}$ below 100 GeV or above 150 GeV).

After the selection of the lepton, it was required that the mass of the remaining particles, forced into 2 jets using LUCLUS, exceeded 30 GeV/c^2, and that each hadronic jet had a multiplicity of 4 or greater with at least one charged particle.

Figure 2 shows the distribution of the momentum of the candidate leptons. The efficiency for the signal selection ($WW \rightarrow q\bar{q}\ell\nu$) was calculated using events generated with PYTHIA 5.7 [10] and using the full detector simulation and was determined to be $(69.4 \pm 1.1)\%$ (90.1, 75.5 and 42.8 for muon, electron and tau events respectively). A correction to the efficiency of -1.0 % has been included to account for the difference in track reconstruction efficiency in data and simulated events and the same amount was added in quadrature to the total systematic error. The expected background cross-section contribution after the selection was estimated to be (0.526 ± 0.079) pb. The errors on the signal efficiency and the background include all systematic uncertainties.

From the full data sample corresponding to an integrated luminosity of 9.98 pb^{-1}, a total of 45 events were selected (17 events with a muon, 14 events with an electron and 14 events with a tau). From this the WW cross-section for semileptonic decays was derived to be

$$\sigma_{WW}^{q\bar{q}\ell\nu} = \sigma_{WW}^{tot} \times Br(WW \rightarrow q\bar{q}\ell\nu) = 5.78\ ^{+1.02}_{-0.93}\ \pm\ 0.17 \text{ pb}\ ,$$

where the first error is statistical and the second systematic. The systematic error has contributions from the uncertainties on the efficiency, the background, the CC03 factor and the luminosity.

4.3 Fully Leptonic Final States

Events in which both W bosons decay into $\ell\nu$ are characterized by two energetic, acollinear and acoplanar leptons of opposite charge, and by large missing energy and momentum. In $W \rightarrow e\nu$ and $W \rightarrow \mu\nu$ decays, the lepton energy ranges typically between 30 and 60 GeV; $W \rightarrow \tau\nu$ decays produce either a single charged particle with a lower momentum, or a narrow jet. The relevant backgrounds are dileptons from $e^+e^- \rightarrow Z(\gamma)$, Bhabha scattering and two-photon collisions. In order to select a sample of purely leptonic events, preliminary cuts were applied to all events, followed by the logical 'OR' of three different selections corresponding to different lepton flavour combinations.

For the preselection, a charged particle multiplicity between 2 and 5 was required with the total energy of these particles greater than 30 GeV, and an acollinearity between the two highest momentum particles in the range $10° < \theta_{acol} < 160°$. All particles in the event were then clustered into jets using the LUCLUS algorithm [8] with $d_{join} = 6.5$ GeV/c and only events with two reconstructed jets were retained, containing at least one charged particle each.

Events from radiative Z production with the ISR photon entering the detector acceptance were explicitly rejected by requiring that there be no neutral energy greater than 10 GeV in a cone with an aperture of 10 degrees around the beam direction. To reduce background from $\gamma\gamma \rightarrow \ell\ell$ events and radiative dileptons events, two further cuts were applied at different values in the three following selections. The first cut was on the angle θ_{miss} between the direction of the missing momentum and the beam direction. For the second cut the 2D-thrust axis was constructed from the projection of the jet momenta

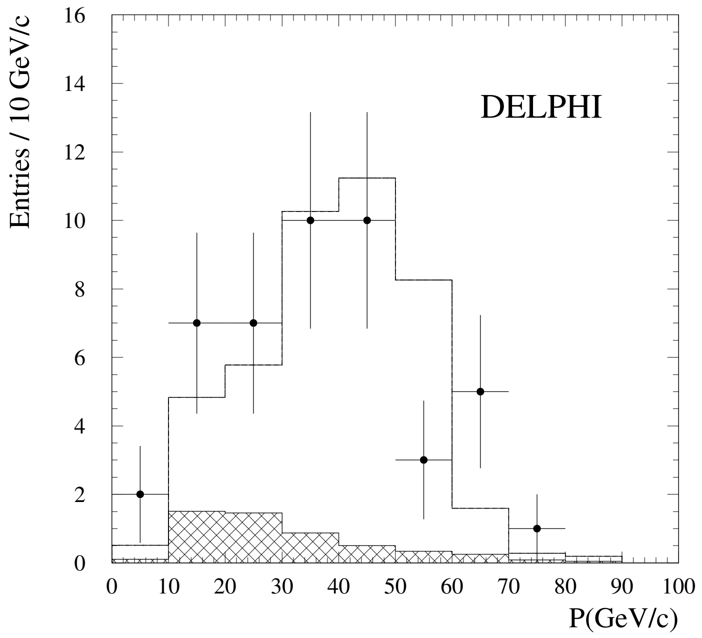

Figure 2: Momentum distribution of the lepton in the semileptonic final states: dots are data and the full line is the SM expectation for the signal (white area) plus the calculated background (cross-hatched area). All cuts were applied except that on the lepton momentum.

into the plane transverse to the beam direction, and the transverse component of the jet momenta with respect to the 2D-thrust axis (p_{tr}) was calculated.

a) e$-\mu$ selection: Events were selected if there was one charged particle with at least 20 GeV of associated electromagnetic energy and one charged particle having a momentum greater than 5 GeV/c and at least a very loose muon identification. The value of $|\cos\theta_{miss}|$ was required to be smaller than 0.98 and p_{tr} was required to be greater than 2 GeV/c.

b) $\mu - \tau$ selection: Events were selected if there was one and only one charged particle with at least a loose muon identification and momentum greater than 20 GeV/c. The momentum of the second jet was required to be greater than 10 GeV/c, $|\cos\theta_{miss}|$ was required to be less than 0.94 and p_{tr} to be greater than 1.2 GeV/c.

c) flavour-blind selection: Events were selected if the momentum of the leading jet was between 25 and 70 GeV/c, that of the other jet between 5 and 60 GeV/c and the total momentum in the plane transverse to the beam direction greater than 8 GeV/c. The electromagnetic energy was required to be less than 110 GeV in total, and less than 70 GeV for a single particle. The value of $|\cos\theta_{miss}|$ was required to be smaller than 0.90 and p_{tr} to be greater than 2 GeV/c.

Figure 3 shows the distribution of $|\cos\theta_{miss}|$. The global efficiency of the selection was estimated to be $(62.6 \pm 2.4)\%$, where a correction of -2.0 % was applied to account for the difference in the track reconstruction efficiency between data and simulated events and the same amount was added in quadrature to the total systematic error. The residual background from non-W and single-W events is 0.133 ± 0.040 pb.

With the criteria described above 8 events were selected in the full data sample. The cross-section for the purely leptonic final states was calculated to be

$$\sigma_{\mathrm{WW}}^{\ell\nu\ell\nu} = \sigma_{\mathrm{WW}}^{tot} \times \mathrm{Br}(\mathrm{WW} \to \ell\nu\ell\nu) = 1.05\ ^{+0.50}_{-0.39}\ \pm 0.09 \text{ pb},$$

where the first error is statistical and the second systematic. The systematic error has contributions from uncertainties in efficiency and background determination, electromagnetic energy calibration, muon identification, evaluation of the CC03 correction factor and the luminosity.

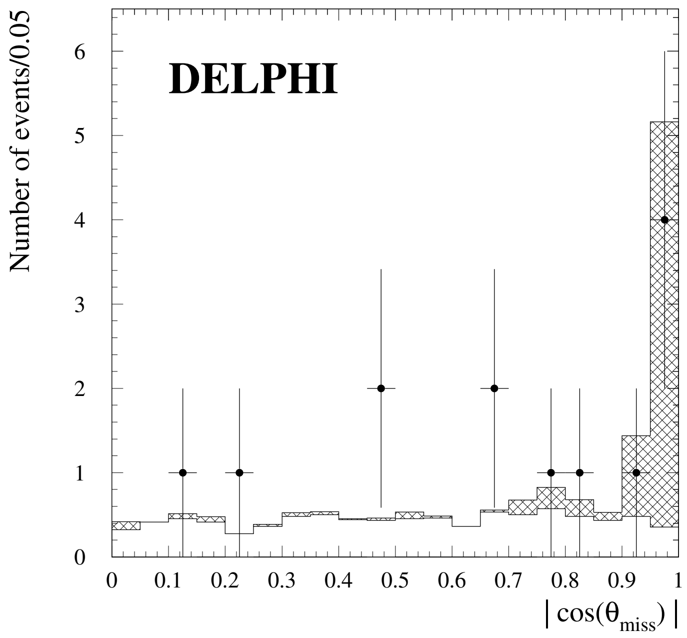

Figure 3: Distribution of $\cos\theta_{miss}$: dots are data and the full line is the SM expectation for the signal (white area) plus the calculated background (cross-hatched area). All cuts were applied except that on $\cos\theta_{miss}$.

4.4 Branching Ratio and Total Cross-section

The total cross-section for WW production and the W branching ratios were obtained from a likelihood fit based on the product of the Poissonian probabilities of finding the observed number of events in the fully hadronic, the three semileptonic and the fully leptonic final states. The results for the leptonic branching ratios are given in table 2 and are consistent with lepton universality. Assuming lepton universality, the fit was repeated including now also the cross-section data obtained at 161 GeV [1]. The result for the leptonic branching ratio is also given in table 2 and the derived result for the hadronic branching ratio $\mathrm{Br}(\mathrm{W} \to \mathrm{q\bar{q}})$ is

$$\mathrm{Br}(\mathrm{W} \to \mathrm{q\bar{q}}) = 0.660^{+0.036}_{-0.037} \pm 0.009$$

where the first error is statistical and the last is systematic. The systematic error is determined from the estimated errors on efficiency and residual background of the different final states.

$\mathrm{Br}(\mathrm{W} \to \mathrm{e}\nu)$	$0.102^{+0.038}_{-0.032} \pm 0.003$
$\mathrm{Br}(\mathrm{W} \to \mu\nu)$	$0.107^{+0.032}_{-0.027} \pm 0.003$
$\mathrm{Br}(\mathrm{W} \to \tau\nu)$	$0.134^{+0.050}_{-0.048} \pm 0.007$
$\mathrm{Br}(\mathrm{W} \to \ell\nu)$	$0.113^{+0.012}_{-0.012} \pm 0.003$

Table 2: Results for the W leptonic branching ratios. The last row shows the W leptonic branching ratio, measured under the assumption of lepton universality. The first errors are statistical, the last are systematic.

The branching ratio is in agreement with the Standard Model expectation of 0.677. An improved measurement of the total cross-section can then be obtained by repeating the likelihood fit with the Standard Model values of the branching fractions imposed. The result is

$$\sigma^{tot}_{\mathrm{WW}} = 11.58\ ^{+1.44}_{-1.35} \pm 0.32 \text{ pb},$$

where the first errors are statistical and the last is systematic.

The evolution of the cross-section as a function of the collision energy is shown in fig. 4 and shows good agreement with the Standard Model prediction.

5 Direct Reconstruction of the W Boson Mass

Above the threshold for W pair-production the W boson mass can be reconstructed directly from its decay products. A priori, the mass resolution obtained from reconstructing m_W from the invariant mass of the $q\bar{q}$ system is not adequate for a precision measurement due to the jet energy resolution. The mass resolution is improved by imposing constraints from momentum and energy conservation. When the two masses are large the constraints induce a large negative correlation between the two measured masses. This leads to an excellent determination of the average of the two masses with a precision at the level of the W width folded with $\mathcal{O}(1\ \mathrm{GeV}/c^2)$.

5.1 Event Selection

The event selections used were simplified versions of those described previously for the cross-section measurement. Emphasis was made on applying only cuts that leave the mass measurement unbiased.

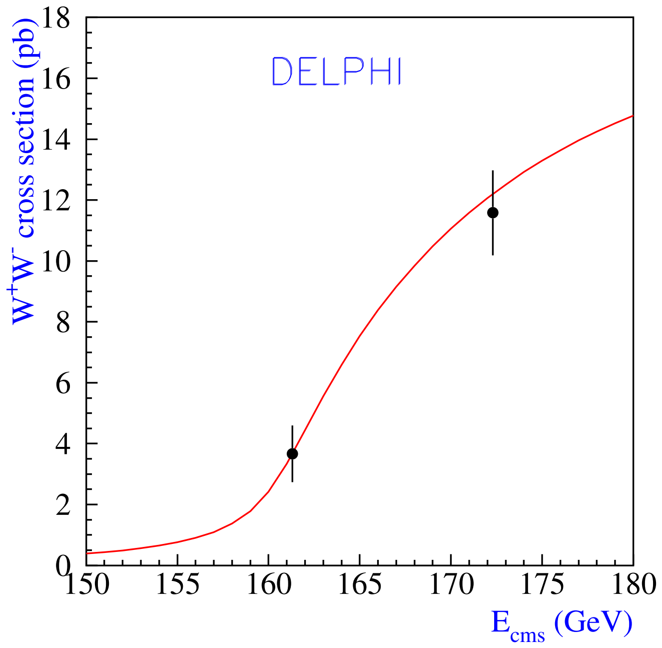

Figure 4: W^+W^- cross-section as a function of centre-of-mass energy. The curve is the Standard Model prediction for $m_W = 80.45$ GeV/c^2.

5.1.1 The Fully Hadronic Channel

The fully hadronic channel has a large background dominated by $q\bar{q}(\gamma)$ events. In order to retain maximal efficiency, only a loose 4-jet selection was applied. Following the event selection, each event was then treated separately with a signal purity estimated on an event-by-event basis.

For each event, all particles were clustered into jets using the DURHAM algorithm [12] with $y_{cut} = 0.001$. Only events with 4, 5, or 6 reconstructed jets were retained. Events with 6 reconstructed jets (5% of the signal) were forced into a 5-jet configuration by raising the value of y_{cut}. The events were subsequently treated according to the number of reconstructed jets, 4 or 5. However, in order to reject events from the $q\bar{q}(\gamma)$ final state, a variable D_{pur} was formed by forcing all events to a 4-jet configuration and then calculating the product of the smallest di-jet opening angle and the minimum jet energy:

$$D_{pur} = \theta_{min} \cdot E_{min}. \tag{2}$$

The purity of an event with a given value of D_{pur} was then estimated as the fraction of events which are coming from the signal as shown in fig. 5.

In order to suppress background with significant initial state radiation the following cuts were used:

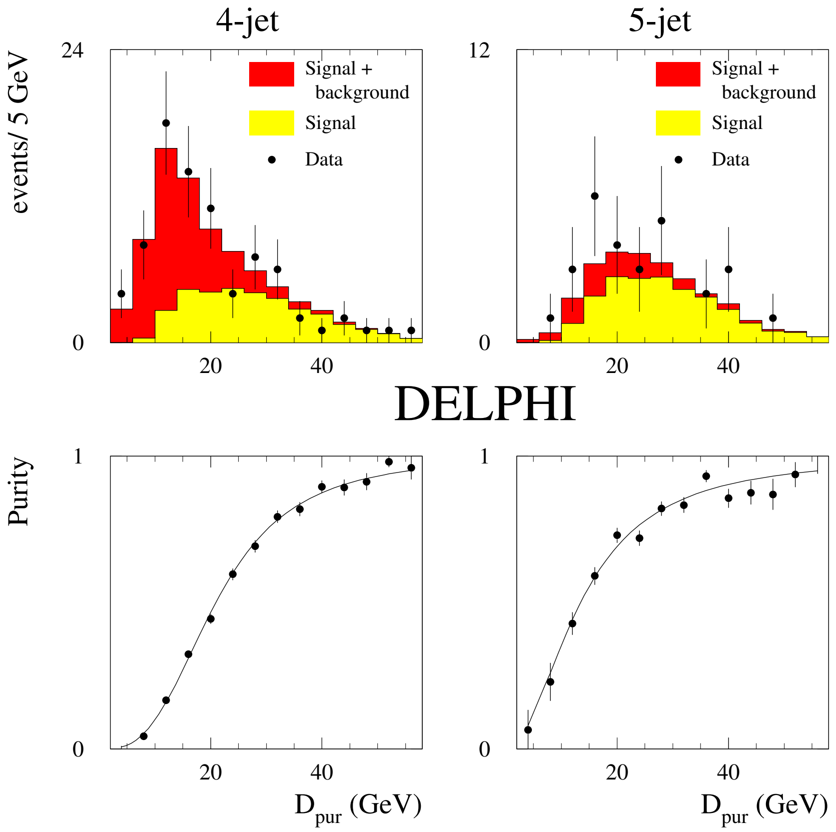

Figure 5: The distribution of D_{pur} for 4-jet and 5-jet events. The lower plots show the purity as a function of D_{pur}. The curves correspond to a simple parametrization.

- The total measured energy was required to be above 93 GeV and the total measured energy of neutral particles less than 130 GeV.
- The charged multiplicity had to be at least 19.
- Jets in both 4-jet and 5-jet events were required to have masses above 1 GeV/c^2 and the number of particles in each jet to be at least 4.
- A 3–C constrained fit (see below) assuming energy and momentum conservation and an undetected photon parallel to the beam direction was required to give an estimate of the photon energy below 25 GeV.

The overall efficiency was found from simulation to be $(89.0 \pm 1.0)\%$ with a residual background of 4.7 ± 0.5 pb, mainly from the $q\bar{q}(\gamma)$ final state.

5.1.2 The Semileptonic Channel

The selection of semileptonic candidates was optimized to keep events where the lepton is a muon or an electron. Events with tau-leptons in the final state were rejected because they contain less information about m_W. The events were selected with the same cuts as for the cross-section measurement except for the following:

- Both electrons and muons were required to be positively identified as described in section 4.2.
- The reconstructed lepton energies were required to be above 23 GeV.
- The isolation of the lepton candidate had to be at least 10 degrees.

After the selection 11 electron and 12 muon candidates remained with a reconstructed mass between 73 and 85 GeV/c^2. The numbers of selected events expected from simulation are 10.3 with 1.0 background in the electron channel and 14.0 with 0.3 background in the muon channel.

5.2 Kinematic Reconstruction

The masses of the events were reconstructed using a constrained fitting algorithm. Each fitted element – lepton, jet or neutrino – is described by three parameters.

Muons are described by their measured momenta and their polar and azimuthal angles. The measurement errors were obtained directly from the track fit with only the momentum error playing any significant role for the precision of the m_W determination.

Electrons are characterized by their measured energies and their detected angular position in the electromagnetic calorimeters. The measurement errors were obtained from parametrizations of the response of the electromagnetic calorimeters, which was tuned to the response found in Bhabha and Compton scattering events. The angular errors were determined from the detector granularity and are significant only for the forward electromagnetic calorimeter.

The fitted jet momentum, $\vec{p_j}^f$, is projected onto a set of axes with one component parallel to the measured jet momentum, $\vec{p_j}^m$, and two transverse components. The first is described by a rescaling factor, $\exp(a_j)$, while the latter is described by two parameters multiplied by perpendicular momenta fixed to 1 GeV/c:

$$\vec{p_j}^f = \exp(a_j)\vec{p_j}^m + b_j\vec{p_j}^b + c_j\vec{p_j}^c \tag{3}$$

The directions of $\vec{p_j}^b$ and $\vec{p_j}^c$ are determined by a method described below.

The jet energy, E_j^m, and thereby also the jet mass is rescaled with the same factor $\exp(a_j)$ as the jet momentum.

The fitting algorithm then minimizes a χ^2:

$$\chi^2 = \sum_j \frac{(a_j - a_0)^2}{\sigma_{a_j}^2} + \frac{b_j^2}{\sigma_{b_j}^2} + \frac{c_j^2}{\sigma_{c_j}^2}, \tag{4}$$

while forcing the fitted event to obey the constraints.

The expected energy loss parameter, a_0, and the energy spread parameter, σ_{a_j}, are parametrized as functions of the angle of the jets with respect to the beam axis, $\cos\theta_j$. The transverse momentum errors depend on how broad the jets are. The broadness of a jet is calculated by projecting the momenta of all the particles belonging to the jet onto the plane perpendicular to the jet axis and forming a 2-dimensional momentum tensor $\mathcal{T}_{\beta\gamma}$:

$$\mathcal{T}_{\beta\gamma} = \sum_k p_\beta^k p_\gamma^k, \tag{5}$$

where p_β^k and p_γ^k are the two components of the projection of the momentum of particle k.

The eigenvectors of the tensor, $\vec{p_j}^b$ and $\vec{p_j}^c$, then give the directions where the jet is broadest and slimmest. The corresponding eigenvalues are B_b and B_c. The transverse momentum errors also depend on how much energy remained undetected in the jet. This quantity, E_{jmiss}, is estimated for each jet by first performing a constrained fit for each event with transverse errors set to 1.5 GeV/c.

The momenta of the primary quark directions from simulated events can be used to estimate the experimental errors on the jet parameters. Hard gluon radiation will however often induce distortions and ambiguities which reduces the performance of this procedure. Instead, the jet errors were tuned so that the analysis produced a pull distribution with a width within 1% of unity. The pull is defined as the reconstructed mass minus the W mass divided by the error, and was evaluated for samples simulated with an integrated luminosity equal to the data.

Since the effects of overlapping jets are more severe in the fully hadronic channel than in the semileptonic channel the tuned jet errors are different in the two cases. For the fully hadronic events:

$$\begin{aligned}
a_0 &= 0.15 + 0.4 \cdot \cos^4 \theta_j \\
\sigma_{a_j} &= 0.27 + 0.72 \cdot \cos^4 \theta_j \\
{\sigma_{b_j}}^2 &= 0.36\, GeV^2 + 1.8 \cdot B_b \frac{\sqrt{1GeV \cdot {E_j}^m + E_{jmiss}^2}}{{E_j}^m} + 0.036\, GeV^{-2} \cdot {B_b}^2 \\
{\sigma_{c_j}}^2 &= 0.36\, GeV^2 + 1.8 \cdot B_c \frac{\sqrt{1GeV \cdot {E_j}^m + E_{jmiss}^2}}{{E_j}^m} + 0.036\, GeV^{-2} \cdot {B_c}^2.
\end{aligned} \tag{6}$$

For the semileptonic events:

$$\begin{aligned}
a_0 &= 0.15 + 0.4 \cdot \cos^6 \theta_j \\
\sigma_{a_j} &= 0.15 + 0.4 \cdot \cos^6 \theta_j \\
{\sigma_{b_j}}^2 &= 0.2\, GeV^2 + 1.0 \cdot B_b \frac{\sqrt{1GeV \cdot {E_j}^m + E_{jmiss}^2}}{{E_j}^m} \\
{\sigma_{c_j}}^2 &= 0.2\, GeV^2 + 1.0 \cdot B_c \frac{\sqrt{1GeV \cdot {E_j}^m + E_{jmiss}^2}}{{E_j}^m}.
\end{aligned} \tag{7}$$

The neutrino momentum vector is considered as unknown, which leads to a reduction of three in the number of constraints. The total χ^2 is then minimized by an iterative procedure using Lagrange multipliers for the constraints.

The value of m_W and its error were calculated from the fitted momenta. Events for which the χ^2 of the fit was larger than the number of degrees of freedom for the fit, NDF, had their errors scaled by a factor of $\sqrt{\chi^2/NDF}$ in order to take non-Gaussian resolution effects into account.

The mass errors depend on the value of the computed masses, which leads to asymmetric errors. In order to correct for this effect, an additional 0.5 GeV/c^2 was added in quadrature to the mass error. This has a small effect on the statistical precision and reduces the bias of the method.

5.3 Extraction of the Likelihood for m_W

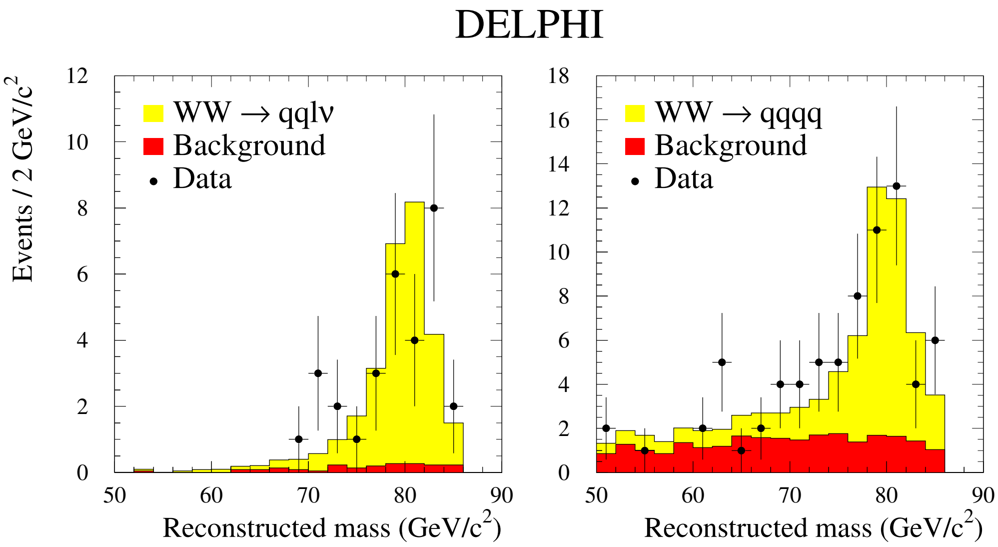

Figure 6: The distributions of the reconstructed masses for the semileptonic and fully hadronic channels.

The resolution on the average of the two reconstructed W masses is found to be much better than that on the difference of the masses. This is due to the negative correlation between the two computed masses. Therefore only one mass was extracted per event. In the constrained fit this was implemented as an additional equal mass constraint. The distributions of the reconstructed mass are shown in fig. 6 for real and simulated data in the semileptonic and fully hadronic channels. For the fully hadronic channel only events with $D_{pur} > 13$ GeV and only the solution with the lowest χ^2 is shown. The treatment of the different solutions in the fully hadronic events is described below.

The information on the W mass was then extracted from the likelihood of observing each individual event. In the case of semileptonic candidates the likelihood is expressed as:

$$\mathcal{L}(m_W) = P\left(\int_0^{E_b} G(m|m_f) \cdot BW(m|m_W) \cdot PS(m)dm\right) + (1-P)p_b(m_f), \qquad (8)$$

where P is the overall fraction of events expected from simulation to be signal (90% for the electron events and 98% for the muon events). $G(m|m_f)$ is a Gaussian resolution function:

$$G(m|m_f) = \frac{1}{\sqrt{2\pi}\sigma_f} \exp(-\frac{(m-m_f)^2}{2\sigma_f^2}), \qquad (9)$$

where m_f is the value of the fitted mass and σ_f is the error on m_f.

$BW(m|m_W) \cdot PS(m)$ is the expected distribution of the average of two W masses:

$$BW(m|m_W) \cdot PS(m) \propto \frac{\Gamma_W}{m_W} \frac{m^2}{(m^2 - m_W^2)^2 + m^4\Gamma_W^2/m_W^2} \sqrt{E_b^2 - m^2}, \qquad (10)$$

where the width of the W resonance is taken as $\Gamma_W = 2.07$ GeV.

The shape of the background distribution, $p_b(m_f)$, was taken numerically from simulation. Only events with a reconstructed mass between 73 GeV/c^2 and 85 GeV/c^2 were used in the semileptonic analysis in order to reject possible non-resonant background events. The integral in eq. 8 was normalized to unity accordingly.

The treatment of the fully hadronic candidates was more involved due to multiple solutions. In the case of 4-jet events there are three ways of choosing a di-jet combination, while 5-jet events lead to 10 possible solutions. However, the measured mass difference can be used to differentiate between the solutions. The fully hadronic candidates were therefore fitted without the equal mass constraint, leading to a mass difference Δ_i with an error σ_{Δ_i} for each possible solution, i. The distribution of the mass difference for the correct solution is a convolution of the experimental resolution and the difference coming from the relativistic Breit-Wigner distributions:

$$p_i \propto \int_{-\infty}^{\infty} \frac{1}{\Delta^2 + {\Gamma_W}^2} \exp\left(-\frac{(\Delta_i - \Delta)^2}{2{\sigma_{\Delta}}_i^2}\right) d\Delta \tag{11}$$

The distribution due to wrong combinations can be assumed to be uniform around zero in the mass difference, so that the relative probability of the solutions can be estimated as p_i. For the 5-jet candidates the relative probability to have gluon radiation was estimated as:

$$p_i^g(k_\perp^g)dk_\perp^g \propto \frac{\alpha_s(k_\perp^g)}{k_\perp^g} dk_\perp^g, \tag{12}$$

where $k_\perp^g$, the transverse momentum of the gluon relative to the quark-antiquark pair which radiated the gluon, was estimated as the minimum $k_\perp$ of the three possible gluon candidates. Each of the ten probabilities was therefore multiplied by $\frac{1}{k_\perp^g}$ and the sum of the probabilities normalized to unity.

In the fully hadronic final state there is a further complication arising from the jet reconstruction procedure not always being able to perform a fully correct clustering. The efficiency, ϵ_c, for a jet reconstruction without major faults was estimated from simulation to be 85% for 4-jet and 75% for 5-jet events. The value of ϵ_c is correlated with the measurement errors described above. The likelihood for observing a fully hadronic candidate is a sum over all the possible solutions:

$$\begin{aligned} \mathcal{L}(m_W) = \sum_i p_i \cdot \Big(P(D_{pur}) \quad \Big[\quad & \epsilon_c\Big(\int_0^{E_b} G(m|m_i) \cdot BW(m|m_W) \cdot PS(m)dm\Big) \\ + \quad & (1-\epsilon_c)p_c(m_i)\Big] + (1 - P(D_{pur}))p_b(m_i)\Big), \end{aligned} \tag{13}$$

where $p_c(m_i)$ (the distribution of the wrong solutions) and $p_b(m_i)$ were extracted from simulation and $P(D_{pur})$ is the event purity described in section 5.1.1.

Since the candidate events are not correlated the combined likelihood for observing all the events is the product of all the event likelihoods. Equivalently, a $\Delta\chi^2$ value can be extracted as:

$$\Delta\chi^2(m_W) = \sum_k -2\ln\mathcal{L}_k(m_W) - \sum_k -2\ln\mathcal{L}_k(m_{W\,max}), \tag{14}$$

where $m_{W\,max}$ is the value of m_W for which the likelihood is largest and the sum is taken over all accepted events. The final likelihood curves are shown in figs. 7 and 8. The fitted

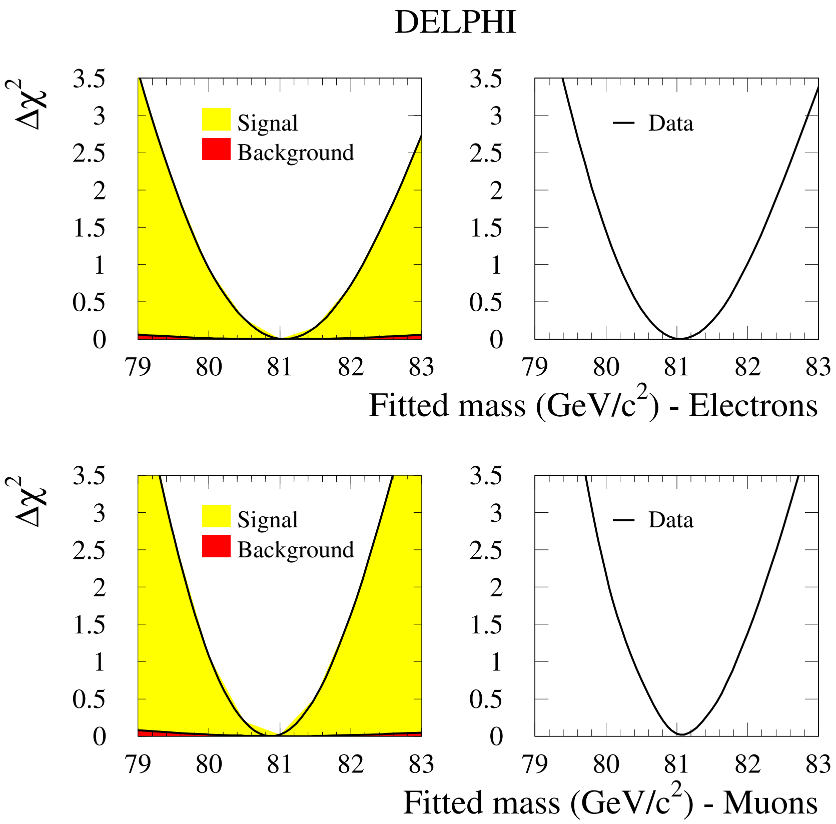

Figure 7: The likelihood curves for the semileptonic analysis. To the right is shown the curve resulting from the analysis of the data while the left hand plots show the average expected likelihood curves from events simulated with $m_W = 80.35$ GeV/c^2.

value of m_W is biased because not all detector and physics effects are taken into account in the likelihood description. In order to correct for this bias a calibration procedure was performed using simulated event samples generated with different values of m_W. The analysis response to the change of m_W is shown in fig. 9. The response is consistent with being linear over the mass range considered and a fit to the expression:

$$m_{rec} - m_{ref} = a(m_{gen} - m_{ref}) + b \tag{15}$$

was used to extract the correction. m_{ref} is the value of the generated mass for which the analysis on simulated events gives a result closest to the data: $m_{ref} = 80.35$ and 79.85 GeV/c^2 for the semileptonic and fully hadronic channels respectively.

The scale factor, a, is slightly below unity which is expected from the effect of initial state radiation. The bias is positive and dominated by two effects; initial state radiation and the measurement errors being negatively correlated with the fitted mass. The latter effect leads to an asymmetric experimental response function which has not been taken into account in the likelihood expression. The statistical errors were checked by performing a large set of simulated experiments and verifying that the observed variance corresponds to the expected one within a precision of 1%. The statistical errors were corrected using

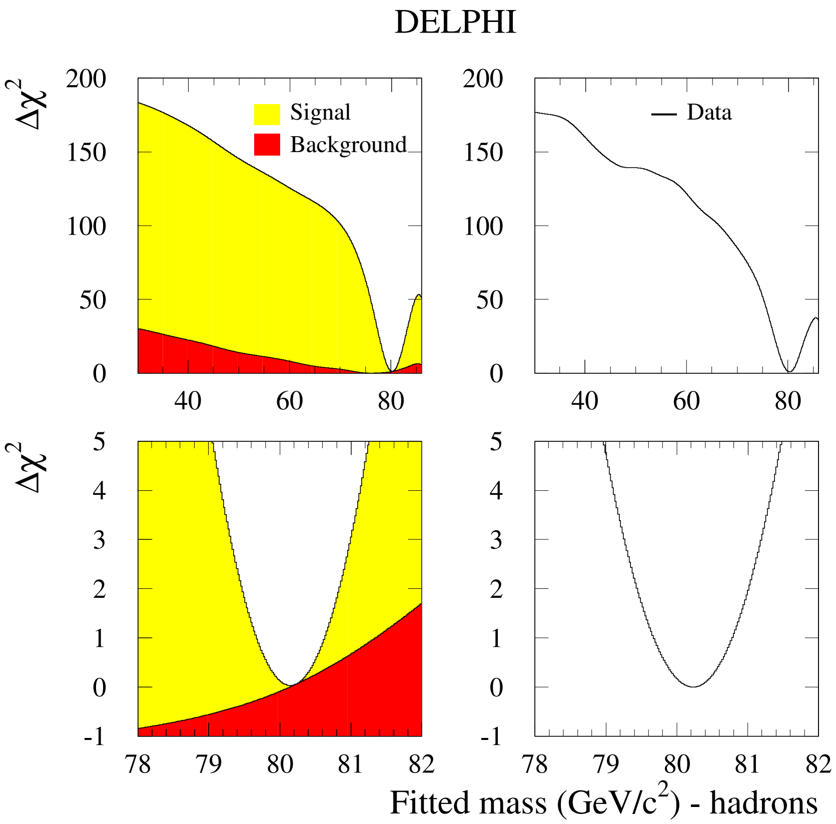

Figure 8: The likelihood curves for the fully hadronic analysis. To the right is shown the curve resulting from the analysis of the data while the left hand plots show the average expected likelihood curve from events simulated with $m_W = 79.85$ GeV$/c^2$. The lower plots show the region around the fitted value of m_W in more detail.

the same scale factor as was applied to the fitted m_W. The final measured values are shown in table 3.

Numerically large statistical fluctuations can be expected in data samples with low statistics. Fig. 10 shows the distribution of errors from samples of simulated fully hadronic events with an integrated luminosity of 9.98 pb^{-1}. Fig. 10 also shows the width of the pull distribution as a function of the likelihood error. It is nearly independent of the error, signifying that the likelihood error can be relied upon.

5.4 Systematic Errors

The analysis described above is to a high degree model independent, but does rely on corrections obtained from simulation. Any error in the simulation will cause a wrong bias and thereby a systematic error.

The systematic uncertainty on the beam energy is slightly above 30 MeV [13] which corresponds to a systematic error on m_W of 30 MeV$/c^2$.

The uncertainties on the correction for the bias are 50, 40, and 25 MeV$/c^2$ for the

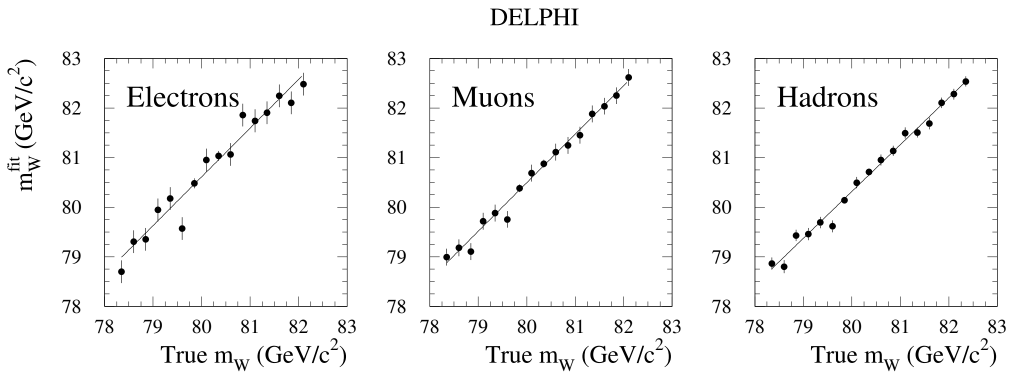

Figure 9: Fitted versus generated W mass for $q\bar{q}e\nu$, $q\bar{q}\mu\nu$ and $q\bar{q}q\bar{q}$ events together with linear fits.

	Electrons	Muons	Hadrons
Expected error on m_W (GeV/c^2)	1.09	0.76	0.52
a	0.97 ± 0.05	0.98 ± 0.04	0.94 ± 0.02
b (GeV/c^2)	0.60 ± 0.05	0.48 ± 0.04	0.33 ± 0.02
Fitted mass on data sample (GeV/c^2)	81.05 ± 0.85	81.04 ± 0.72	80.23 ± 0.56
Measured W mass (GeV/c^2)	**80.45±0.87**	**80.56±0.76**	**79.90±0.59**

Table 3: Results of the analysis of the $q\bar{q}e\nu$, $q\bar{q}\mu\nu$ and $q\bar{q}q\bar{q}$ channels. The expected error is after calibration. a is the scale factor from the calibration procedure and b is the bias from analysis. The measured value of m_W is given before and after the calibration correction.

electron, muon and fully hadronic channels. These errors come from limited simulation statistics and are uncorrelated between channels.

The possible systematic error from the description of the response of the DELPHI detector has been evaluated using the Z^0 data collected during the 1996 data taking. Discrepancies between the energy flow measurement in hadronic decays were evaluated and parametrized as a function of the polar angle. These discrepancies were then implemented in the simulated events. This leads to changes in the bias of up to 30 MeV/c^2 which has been used as a systematic error. This error is taken as being fully correlated for the electrons and muons while only half of the effect is correlated between the semileptonic and fully hadronic channels. This is due to the different impact of the jet energy measurement after the constrained fit.

The uncertainty on the muon momentum was estimated from $Z^0 \to \mu^+\mu^-$ events to be 0.5%, while the Bhabha and Compton scattering events showed an uncertainty on the electron energy of 1%. This corresponds to uncorrelated systematic errors of 10 and 15 MeV/c^2 respectively.

The impact of an incorrect description of the jet fragmentation is estimated to have negligible consequence for the semileptonic channels. This leads to an estimated fully

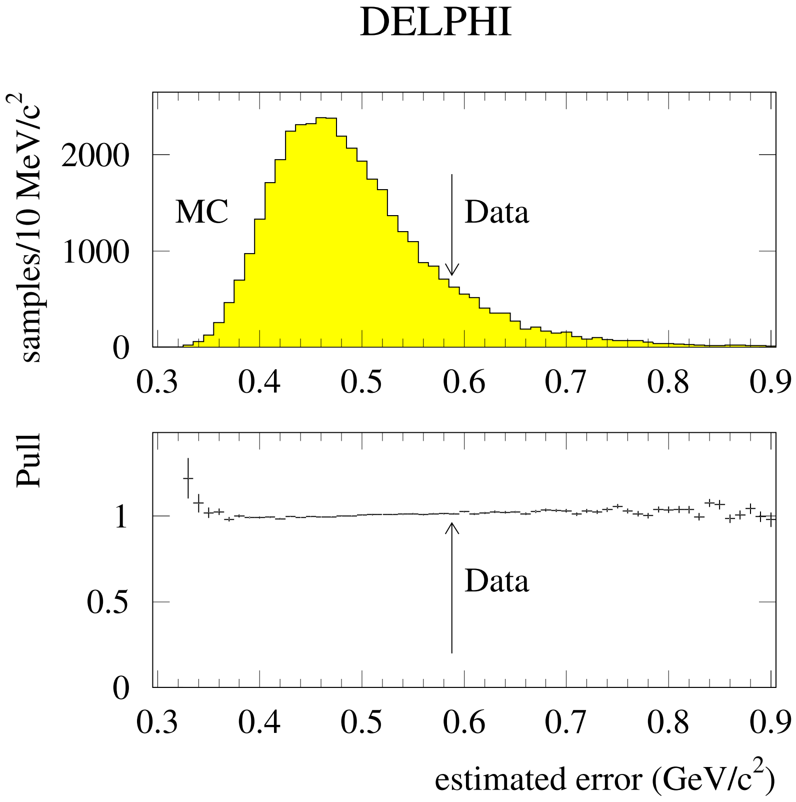

Figure 10: The distribution of errors from samples of simulated hadronic events. The upper plot shows the distribution. The lower plot shows the width of the pull distribution as a function of the error. The arrow indicates the value of the likelihood error from the data.

correlated systematic error on m_W of 10 MeV$/c^2$. For the fully hadronic channels the situation is less clear due to the overlap of jets from different W decays. This error was studied by looking at the difference between two simulated samples generated with JETSET [10] and ARIADNE [14], which have different treatment of the parton shower, and used in conjunction with a simplified simulation of the DELPHI detector. A difference in m_W of 2 ± 25 MeV$/c^2$ was found, where the statistical error is taken as a systematic error.

The impact of the background on the semileptonic channel is very small and a change of $\pm 10\%$ leads to correlated changes of 5 MeV$/c^2$ in the bias, which is taken as the systematic error. The background plays a more important part in the fully hadronic analysis, but the inclusion of event-by-event purity leads to a small effective impact. Leaving out the background totally changes the bias by 90 MeV$/c^2$. The systematic error on the level of background leaves a systematic uncertainty of 10 MeV$/c^2$, while the difference between the JETSET and ARIADNE Monte Carlo generators was used to estimate an uncertainty of 10 MeV$/c^2$ coming from the shape of the background mass distribution.

In addition to the W pair-production via the CC03 diagrams, the four-fermion final states may be produced via other electroweak diagrams involving either zero, one, or two massive vector bosons. The effects of the interference between the CC03 diagrams and the additional diagrams were estimated at generator level. Except for the electron channel the effect was found to be negligible and a systematic error of 10 MeV/c^2 was estimated. The electron channel is more affected due to the interference with the single W production leading to a positive shift of 50 MeV/c^2 at the generator level when the mass was estimated from a lineshape fit. A simplified detector study on this channel gave compatible results. The fitted value of m_W was corrected for this effect in the electron channel and a systematic error of 50 MeV/c^2 was assigned.

The systematic error coming from the uncertainty of the simulation of initial state radiation was assigned to be 10 MeV/c^2 [7], fully correlated between the channels.

5.4.1 Interconnection Effects

At the collision energies which can be reached at LEP2, the W bosons are typically separated by $\mathcal{O}(0.1$ fm$)$ when they decay. This is much smaller than the typical hadronisation scale and interactions between the two systems can therefore influence the W mass distribution in the case where both W bosons decay hadronically. Two potentially significant effects have been identified: Colour reconnection in the non-perturbative stage of hadronisation [15, 16] and Bose-Einstein correlations among identical bosons from the two W bosons [17].

In the case of colour reconnection, several phenomenological studies have been performed [16, 18, 19, 20, 21], but the results are so far somewhat inconclusive. We therefore for the time being assign a systematic error of 100 MeV/c^2 from this source [22]. A study claiming the possibility of a substantially larger effect [23] also predicts a substantial decrease in the multiplicity [24], which is disfavoured by the data [25].

For Bose-Einstein correlations, the first study [17] indicated possible effects on the W mass of the order of 100 MeV/c^2, but newer studies [26, 27] give much smaller effects, in part due to the realization that the value of the mass determined from a fit to the lineshape is much less sensitive to the effect than the average mass considered in [17]. A systematic error of 20 MeV/c^2 is therefore assigned due to this effect.

All the systematic errors for each of the channels and combination of channels are finally shown in table 4.

6 Combined Measurement of m_W

Combining the results from the two semileptonic decay channels yields:

$$m_W = 80.51 \pm 0.57(stat.) \pm 0.05(syst.) \pm 0.03(LEP)\, GeV/c^2.$$

Combining the result from the semileptonic decay with the hadronic yields:

$$m_W = 80.22 \pm 0.41(stat.) \pm 0.04(syst.) \pm 0.05(int.) \pm 0.03(LEP)\, GeV/c^2,$$

where int. stands for the interconnection effects.

The cross-section for $e^+e^- \to W^+W^-$ near threshold is also sensitive to the value of m_W which can therefore be estimated. Such an estimate is only valid within the Standard

Channel Source of systematic error	Electrons	Muons	Semi- leptonic	Fully hadronic	All Combined
Calibration	50	40	31	25	20
Detector jets	30	30	30	30	26
Lepton energy	15	10	9	0	5
Fragmentation signal	10	10	10	25	13
Fragmentation background	0	0	0	10	5
Level of background	5	5	5	10	6
4-fermion correction	50	10	22	10	12
ISR	10	10	10	10	10
Colour reconnection	0	0	0	100	48
Bose-Einstein	0	0	0	20	10
Beam energy	30	30	30	30	30
Total error (MeV/c^2)	**85**	**62**	**60**	**116**	**70**

Table 4: A breakdown of the systematic errors from the direct reconstruction of m_W.

Model. The cross-section measurement obtained at 161 GeV [1] was combined with the value obtained at 172 GeV which is less sensitive to m_W. The procedure was identical to the one used for extracting the value of m_W at 161 GeV. The combined value of the W-boson mass was then determined to be:

$$m_W = 80.45 \pm 0.43(stat.) \pm 0.09(syst.) \pm 0.03(LEP)\, GeV/c^2.$$

Combining the W mass obtained from the cross-section measurement with the direct reconstruction result yields:

$$m_W = 80.33 \pm 0.30(stat.) \pm 0.05(syst.) \pm 0.03(int.) \pm 0.03(LEP)\, GeV/c^2.$$

7 Summary

From a data sample of 9.98 pb^{-1} integrated luminosity, collected by DELPHI at a centre-of-mass energy of 172 GeV the branching ratio $Br(W \to q\bar{q})$ was measured to be $0.660^{+0.036}_{-0.037}(stat.) \pm 0.009(syst.)$ and the cross-section for the doubly resonant process $e^+e^- \to W^+W^-$ to be $11.58^{+1.44}_{-1.35}(stat.) \pm 0.32(syst.)$ pb. The mass of the W boson has been obtained from direct reconstruction of the invariant mass of the fermion pairs in the decays WW $\to \ell\nu q\bar{q}$ and WW $\to q\bar{q}q\bar{q}$: $m_W = 80.22 \pm 0.41(stat.) \pm 0.04(syst.) \pm 0.05(int.) \pm 0.03(LEP)\, GeV/c^2$, Combined with the W mass obtained from the cross-sections measured by DELPHI, a value of $m_W = 80.33 \pm 0.30(stat.) \pm 0.05(syst.) \pm 0.03(int.) \pm 0.03(LEP)\, GeV/c^2$ is found.

Acknowledgements

We thank the SL division of CERN for the excellent performance of the LEP collider and their careful work on the beam energy determination. We are also grateful to the technical and engineering staffs in our laboratories and to our funding agencies for their continuing support.

References

[1] DELPHI Collaboration: P. Abreu et al., Phys. Lett. **B397** (1997) 158.

[2] DELPHI Collaboration: P. Aarnio et al., Nucl. Instr. & Meth. **A303** (1991) 233.

[3] DELPHI Collaboration: P. Abreu et al., Nucl. Instr. & Meth. **A378** (1996) 57.

[4] DELPHI Collaboration: *DELPHI event generation and detector simulation - User Guide*, DELPHI Note 89-67 (1989), unpublished.

[5] A. C. Benvenuti et al., *The DELPHI Small Angle Tile Calorimeter*, contribution to IEEE NSS 1994.

[6] S. Jadach, O. Nicrosini et al., *Event Generators for Bhabha Scattering*, Physics at LEP2, eds. G.Altarelli, T.Sjöstrand and F.Zwirner, CERN 96-01 (1996) Vol 2, 229.

[7] W. Beenakker, F. A. Berends et al., *WW Cross-Section and Distributions*, Physics at LEP2, eds. G. Altarelli, T. Sjöstrand and F. Zwirner, CERN 96-01 (1996) Vol 1, 79.

[8] T. Sjöstrand, *PYTHIA 5.7 / JETSET 7.4*, CERN-TH.7112/93 (1993).

[9] P. Abreu, D. Fassouliotis, A. Grefrath, R.P. Henriques and L. Vitale, *SPRIME, A Package for Estimating the Effective* $\sqrt{s'}$ *Centre of Mass Energy in* $q\bar{q}(\gamma)$ *Events*, internal DELPHI note 96-124 PHYS 632 (1996), unpublished.

[10] T. Sjöstrand, *PYTHIA 5.719 / JETSET 7.4*, Physics at LEP2, eds. G. Altarelli, T. Sjöstrand and F. Zwirner, CERN 96-01 (1996) Vol 2, 41.

[11] DELPHI Collaboration: P. Abreu et al., Z. Phys. **C73** (1996) 11.

[12] S. Catani et al., Phys. Lett. B269 (1991) 432;
N. Brown and W. J. Stirling, Z. Phys. C 53 (1992) 629.

[13] The working group for LEP energy, *LEP Energy Calibration in 1996*, Lep Energy Group/97-01 (1997).

[14] L. Lönnblad, Comp. Phys. Comm. 71 (1992) 15.

[15] G. Gustafson et al., Phys. Lett. B209 (1988) 90.

[16] T. Sjöstrand and V. Khoze, Phys. Rev. Lett. 72 (1994) 28;
T. Sjöstrand and V. Khoze, Z. Phys. C 62 (1994) 281.

[17] L. Lönnblad and T. Sjöstrand, Phys. Lett. B351 (1995) 293.

[18] G. Gustafson and H. Häkkinen, Z. Phys. C 64 (1994) 659.

[19] B. Webber in *QCD event generators*, ed. I. G. Knowles and T. Sjöstrand, in CERN 96-01 (1996).

[20] L. Lönnblad, CERN-TH/95-218 (1995).

[21] S. Todorova in *QCD event generators*, ed. I. G. Knowles and T. Sjöstrand, in CERN 96-01 (1996).

[22] Z. Kunszt and W. J. Stirling et al., *Determination of the mass of the W boson* in CERN 96-01 (1996) Vol. 1, 141–205, eds. G. Altarelli, T. Sjöstrand and F. Zwirner.

[23] J. Ellis and K. Geiger, Phys. Rev. D54 (1996) 1967.

[24] J. Ellis and K. Geiger, CERN-TH/97-46.

[25] *Charged Particle Multiplicity in* $e^+e^- \rightarrow q\bar{q}$ *events at 161 and 172 GeV and from the decay of the W Boson.*
DELPHI Collaboration: P. Abreu et al.,
To be submitted to Phys. Lett. B

[26] V Kartvelishvili, R. Kvatadze and R. Møller, MC-TH-97/04-rev, hep-ph/9704424

[27] S. Jadach and K. Zalewski, CERN-TH/97-29.